Evaluation of the Multispectral Satellites with Object-Based Classifiers for Land Use and Land Cover Classification

Eman A. Alshari[1,2(✉)] and Bharti W. Gawali[2]

[1] Computer Science and Information Technology Department, Thamar University, Dhamar, Yemen
em.alshari3@gmail.com

[2] Dr. Babasaheb Ambedkar, Marathwada University, Aurangabad 431004, India

Abstract. This research aimed to evaluate traditional machine learning to achieve high-resolution LULC classification with multispectral satellites and object-based classifiers. Multispectral satellites have high importance in getting and downloading images of observation land. This article describes the comparative analysis of Sentinel-2A (10 m resolution) and Landsat8 (30 m resolution)Satellites with two classifiers from object-based machine learning methods, Random Forest (RF) and K Nearest Neighbor (KNN), to experiment with the classification of five years (2015, 2016, 2017, 2018, and 2019) with 95 images downloaded, 60 images with sentinal2A, and 35 images with landsat8. Area of Sana'a region. This Study indicated that Random Forest proved efficient for Sentinel 2A and Landsat8. Whereas KNN worked well with Landsat8 and provided higher accuracy than RF. The interpretation of these results may be due to the RF classifier requiring many features for good accuracy. At the same time, KNN works well with a small number of input feature variables and gives good accuracy.

Keywords: Multispectral Satellites · Land Use & Land Cover Classification (LULC C) · Sentinel-2A satellite (10m) · Landsat8 Satellite (30m) · Random Forest (RF) Classifier · K-Nearest Neighbour (KNN) · Sana'a City

1 Introduction

Multispectral sensors are stimulated by incoming energy reflected or released by things on the land's surface, diffused, and collected in sensors sensitive to a wide range of spectral bands [1]. These spectral bands are represented by a small section of the electromagnetic spectrum specified by the sensor's shortest and most effective wavelengths, resulting in a single bitmap for each spectral band. Figure 1 shows the four most often utilized spectral bands in open data multispectral satellite missions worldwide, with black boxes indicating incoming intensity. Optical imaging technologies include near-infrared imaging systems [2].

The energy of the sensor is converted into digital data, which is affected by the weather conditions at the time of measurement. As a result, rather than a quantifiable

R. Manza et al. (Eds.): ACVAIT 2022, AISR 176, pp. 602–625, 2023.
https://doi.org/10.2991/978-94-6463-196-8_46

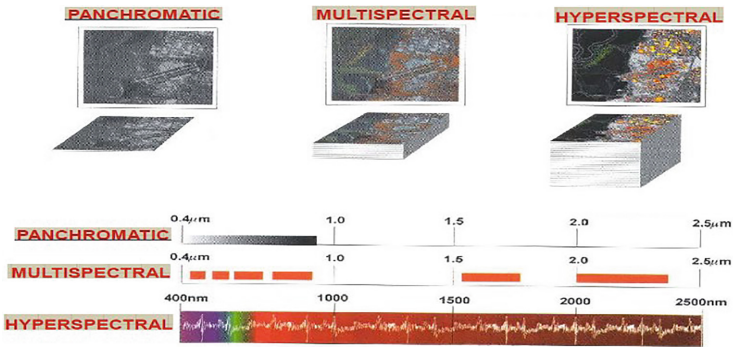

Fig. 1 Types of optical imaging systems and Spectral Resolution Concepts

physical unit, the numerical value indicates the relative relationship of the reversal at the time of observation [3]. It's required to translate numerical figures into an inversion, which is the ratio of the energy reflected for each spectral band to the overall power the sensor receives while analyzing this data. Spectral differences are used to identify and characterize land cover. Every spectral range has its unique personality [4]. When contrasted to the rest of the land, each cover feature has its unique spectral signature, defined by a considerable change in reflectance in one or more spectral bands, as shown in (Fig. 2).

High-resolution satellite images are limited compared to multispectral images in developing countries. This Study compares multispectral satellites using robust accuracy classifiers, Random Forest and KNN. The Pros of multispectral satellites are that it offers a significant number of free imagery: The images' spatial resolution varies (10500 m / pixel). As a result, these satellites may be utilized to get a large area at no cost. The concept is low-cost, easy to implement, and rapid. Significant differences between Landsat8 and Sentinel-2 may have a role in this Study's results. For example: Visiting time Landsat8 16 days and Sentinel-2 ten days per satellite, five days for two satellite constellations. It may be possible to be influenced by this difference from the workbook. Visiting time Sentinel-2 ten days per satellite maybe was not suitable with characters KNN that was my opinion [10].

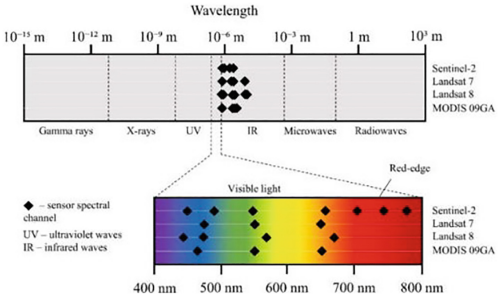

Fig. 2 Comparison of spectral bands for several multispectral satellites.

The machine learning algorithms effectively utilize the sensor images for land cover classification like Random forest and KNN [11]. RF is a collection or group of Classification and Regression Trees created through random resampling on the preparation set on datasets of comparable size to the preparation set, known as bootstraps. It is capable of accurately classifying large amounts of data. It is a learning system built with many decision trees during training, and the individual trees anticipate the modal output [12]. It has become a choice of researchers for classification, prediction, investigating variable importance, and variable selection [13]. The K-Nearest Neighbour method is one of the most fundamental Machine Learning algorithms. It is an approach that saves all available data and categorizes new data points depending on their similarity to the current data. Further data may be swiftly sorted into a well-defined category utilizing the approach [14].

The software used in this study is QGIS and SAGA GIS, a free, open-source software Automated Geoscientific Analysis. SAGA is a GIS application of spatial algorithms which are simple and effective. It includes an easy-to-use user interface with various visualization possibilities and a rich, increasing collection of geoscientific methodologies [15].

This Study attempted to work on the classification of LULC that depends on several factors to obtain a high-resolution characterization and varies according to the classifier used, the image, the time of filming, and the weather conditions in which it was captured., etc. The results showed that selecting only high-resolution satellite images is not enough. The characteristics of the classifier have a significant role in obtaining high-accuracy results in classification. This Study also presented that compatibility of the type of satellite with the typical characteristics of the classifier chosen is critical, which means that the specific features of the classifier selected are essential for this satellite. All of these factors have a role in achieving high-accuracy classification results. The significance of the Study lies in applying multispectral satellites under certain conditions and coming up with significant results. This research will be a helpful way to reveal to new researchers a way to obtain high accuracy in classifying changes in land use and land cover. And it helps specialists in this field decide on the selection type of method and type of satellite and Search in the development of traditional machine learning. This article will effectively plan the future aspects of LULC. This research presented the following: It compared two types of multispectral satellites (Landsat8 and Sentinel-2A) with two object-based classifiers (KNN and RF) of machine learning. It created a database or references for LULC of Sana'a city, the capital of Yemen, consisting of five years (2015, 2016, 2017, 2018, and 2019) with 95 images downloaded, 60 images with sentinal2A, and 35 images with landsat8. The Study presents the experimentation result of two satellite images with machine learning for Sana city –Yemen's capital- which is not yet explored with this approach. The result will assist in monitoring and predicting future land use and cover changes.

2 Literature Review

The summary of the literature survey, this study has concentrated on analyzing the performance of the multispectral satellites presented by research efforts in recent years [16–30]. It focused intensely on factors that influence their performance. This Study dealt with about forty-six studies analyzed systematically. They deal with pixel-based classifiers and other techniques but did not study multispectral satellites with object-based classifiers like this Study in explanation, analysis, and comparisons. Previous studies indicated the gap in studying land change classification with sentinel-2A and landsat8 satellites. In (Fig. 3) has cleared the research line about pixel-based and other techniques with the sentinel-2A versus landsat8 in recent years. The results of these studies show that little research supports that Landsat8 Satellite (30 m) is better than Sentinel2A (10m) [16]. But there are significantly more studies supporting that Sentinel2A (10m) was better than Landsat8 Satellite (30 m) [22–30]. Their findings reveal that the Sentinel2A (10 m) satellite has a superior resolution to the Landsat8 satellite. Their output was that Sentinel2A (10m) is better than Landsat8 Satellite [23] is logical because the pixel classifiers are affected by the location of the images sure gives high accuracy with Sentinel-2A -10-m more than Landsat8 Satellite (30 m). The review of work in this study also revealed that, despite the high resolution of deep learning, machine learning is still widely used and continues to be used today, with classical machine learning outperforming deep learning in terms of features and characteristics. Machine learning is less time-consuming and more accessible to implement than deep learning [29, 30]. The study demonstrated that it is possible without deep learning, we could have achieved a very high resolution for LULC classification using traditional machine learning and multispectral satellites [31–35].

Through Recent Years for pixel-based classifiers.

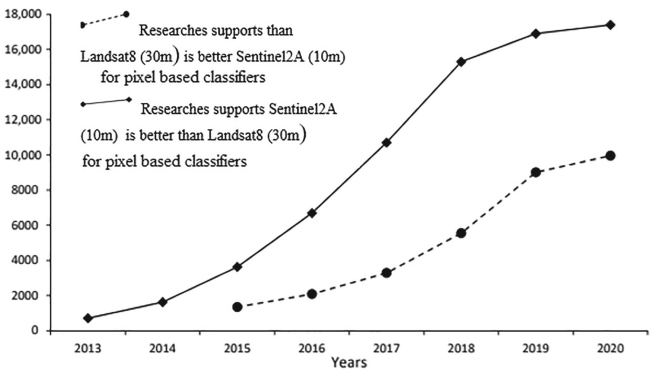

Fig. 3 Research Line Path About The Sentinel2A (10m) Versus Landsat8 Satellite (30m)

2.1 Limitation of This Study

To achieve the high-resolution classification of land changes using multispectral satellites and machine learning in a manner that competes for deep learning and high satellite. It was necessary to study the limitations of methods and satellites used in this Study during the survey literature review. There are essential details for the restriction of Landsat8 and Sentinel-2 described in (Table 1). The limitation of the methods used in this study is mentioned in detail in (Table 2 and Table 3).

Table 1. Differences between Sentinel-2A and Landsat8

Limitation	**Landsat 8**	**Sentinel-2**
Bands	Eight color	13 (3 red edge bands have some vegetation and chlorophyll in the ocean, applications)
Thermal bands	2 (band ten is generally better)	None
Swath width	185 km	290 km
Inclination (angle orbit crosses equator)	98.22	98.56
Best spatial Resolution	15 m pan, 30 m MSI	10 m for four bands
Revisit time	16 days	Ten days per satellite, five days for the constellation with two satellites
Coverage limits	81.8 S to 81.8N	systematic coverage: 56S to 84 N
		on request to 84S
Recorded data:	16-bit DN, which can be linearly scaled to TOA radiance or reflectance using constants in metadata	16-bit DN, which can be converted to TOA reflectance by dividing by 10000
Resolution of space (m)	(15),30,100	10,20,60
Temporal reorganization (days)	16	2–3
Resolution of spectral data	11 bands	13 bands
Resolution in radiometric terms	16-bit	12-bit
Width of the swath (km)	185	290
Range of wavelengths (nm)	433–12,500	442–2186
The scale of supported investigations is large.	National,Regional	Local, National

Table 2. Differences between Pixel and Object-based

No	**Pixel-based**	**Object-based**
1	The image is classed using spectral information in the pixel-based technique, which is frequently used to extract low-level characteristics. Because the classes are unclear, the pixels in the overlapped region will be incorrectly identified.	The aggregation of picture pixels into spectrally homogenous image objects ensures that the pixels not in an overlapping region will not be misclassified due to the object-based approach, frequently used to extract high-level features from images.
2	Only spectral data (pixel intensity) is used as a training set.	First, using spectral and geographical data (neighborhood pixels) as a training set
3	The techniques directly classify a single pixel.	After first aggregating image pixels into spectrally homogenous things, approaches classify individual objects using an image segmentation algorithm.

3 Materials and Procedures

3.1 Area of Study

Sana'a is Yemen's capital and the administrative seat of the Sana'a Governorate. Sana'a is situated at an altitude of 2150 m above sea level, on the line (15–21) north of the equator and longitude (12–44) east of Greenwich. It is surrounded by two mountains (Jabal Naqum on the east and Jabal Eiban on the west) and the province [36]. The city boasts a unique setting at roughly 2,200 m above sea level [37]. Sana'a is Yemen's largest city and the Governorate's administrative center. The elevation is 2,300 m (7,500 ft). It is the country's highest capital and is near the Sarawat Mountains. It has a population of roughly 3,937,500 (2012)[19]. It covers about 17,707.214 km2 land area in this study (Fig. 4).

3.2 Methodology

A brief explanation of the methodology for processing satellite data is shown in Fig. 5.

3.3 Pre-processing for LULC Classification

It is the primary and essential task in the process LULCC, the coordinate reference system for defining and cutting the map into specific areas. The pre-processing process procedure includes studying the location of the case study exactly, as evident in this study (Fig. 6), and identifying the data after being downloaded from satellites under remote sensing technology precisely (Figs. 7 and 8). The information subject to pre-processing is divided into the images shown in WGS84 or WGS84 / UTM.

Multispectral images from Sentinel-2 and landsat8 are available for the case study (Figs. 7 and 8), showing the pre-processing corrections for band 432. The pre-processing contains valid data with a geometric and radiometric correction, presented in this study

Table 3. Differences between RF and KNN

No	**RF**	**KNN**
1	RF classifier is object-based and hyper-parameter.	KNN classifier is object-based. Its algorithm is nonparametric, meaning it doesn't make assumptions about the data.
2	It depends on identifying objects without going into the details of those objects.	It's also known as a lazy learner algorithm since it doesn't immediately learn from the training set; instead, it keeps the dataset and performs a task.
3	It is known as neural networks, which provide estimates for variable relevance.	This method merely saves the information during the training phase. When it receives new data, it classifies it into a category similar to the latest data.
4	It also offers a preferable way of dealing with data that is missing.	Benefits of the KNN Algorithm: It is simple to implement. It can cope with noisy training data. It may be more successful if the training data is vast.
5	Its approach can also handle large datasets with thousands of variables. When a class is rarer than other classes, it can automatically balance data sets.	Disadvantages of the KNN Algorithm: The value of K must constantly be determined, which might sometimes be challenging. The computation cost is high since the distance between the data points for all training samples must be selected [16].
6	The method works quickly with variables suited for more complex jobs [21].	It predicts the output of data points using a labeled input data set. It's one of the most basic Machine Learning algorithms and may be used for a wide range of issues.
7	Missing values are filled in by the variable that appears the most in a given node.	The KNN technique is substantially quicker than earlier training-based algorithms [37].
8	It is implemented using algorithms with built-in feature selection techniques [34].	It's primarily based on visual resemblance.
9	It is effective because they have solid predictive performance, little overfitting, and is simple to comprehend [34].	The training data is saved and only used to produce real-time predictions to learn from it.

[37] with QGIS and SAGA software. These operations improve satellite imagery for classification and rectify the degraded image to generate a more authentic portrayal of the actual scene [37].

3.4 Classification Methods Used in This Study

There are four groups for classification models. Every group contains five categories of the models for five years, 2015, 2016, 2017, 2018, and 2019, as described in

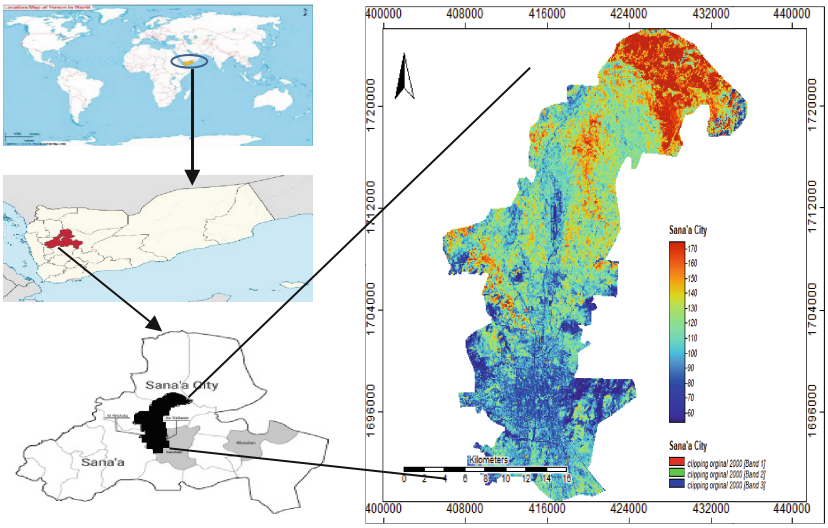

Fig. 4 The location of Sana'a City Study area

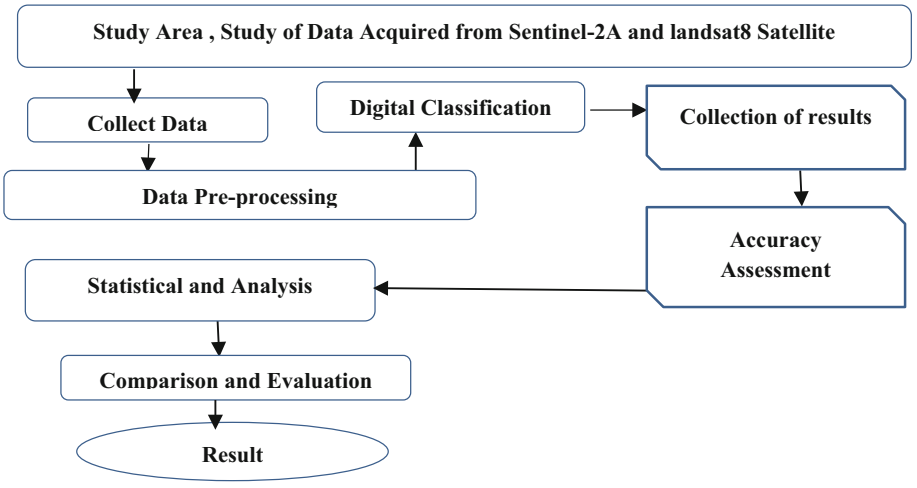

Fig. 5 Workflow Diagram For Proposed Methodology

(Figs. 9, 10, 11, and 12). Twenty images are selected from the found 95 pictures of the database for twenty proposed models to train, validate, and test the methods, five models for landsat8 with RF, five models for landsat8 with KNN, and five models for sentinel-2A with RF, and five models for sentinel-2A with KNN. The band classification used in this study is RGB 432. There are six samples and six parameters for creating model classes: High Land, Mountains, Land Area, Built-up, Vegetation, and Bare Land. Create the samples depending on RGB color composites of Landsat & sentinel-2A satellites, for example, the class Vegetation (red pixels in color composite RGB = 432). This

Fig. 6 Sana'a area on google map

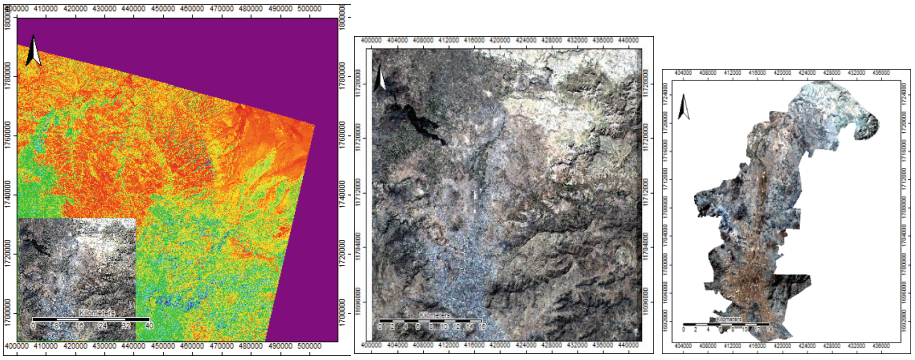

Fig. 7 Data set of Sentinel-2A Satellite Sensor with selection and clipping of area study in Composite

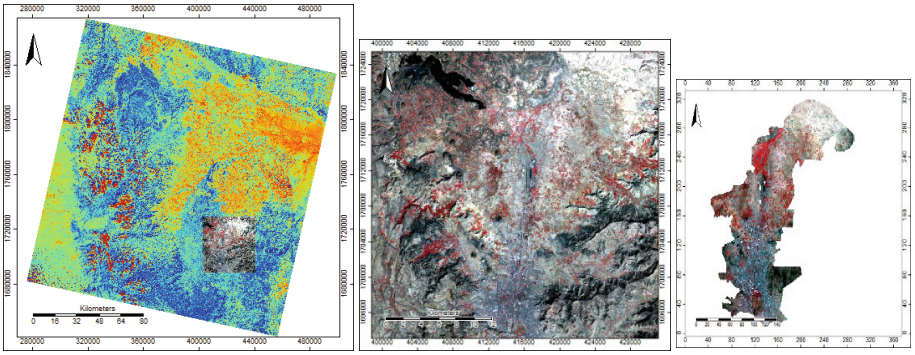

Fig. 8 Data set of Landsat8 Satellite Sensor with selection and clipping of area study in Composite band 432

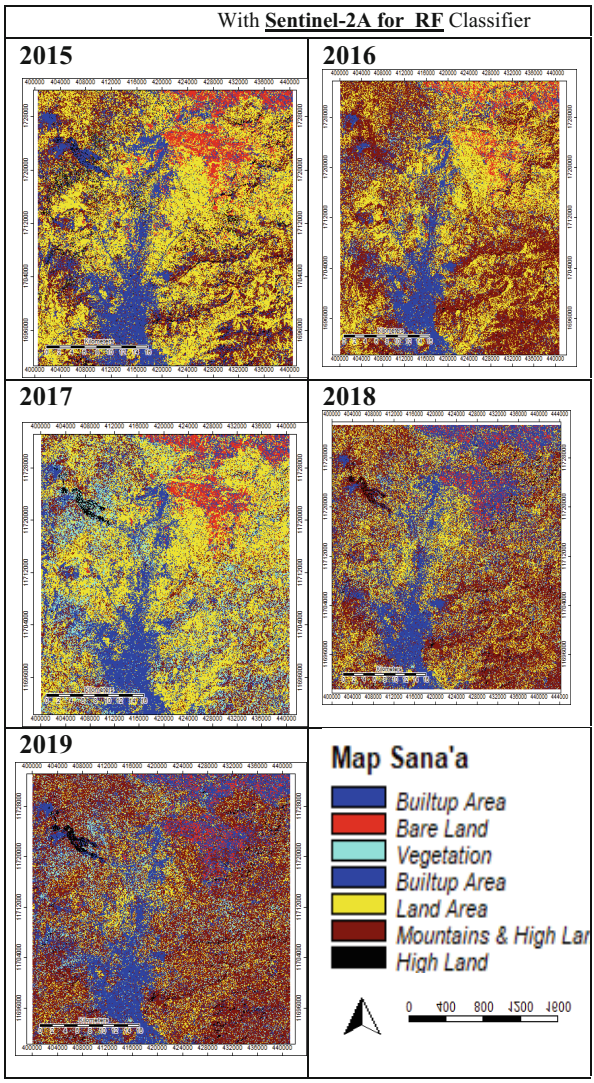

Fig. 9 Group1 of LULC Classification From 2015 To 2019 With **Sentinel-2A for RF** Classifier

article reveals methodology followed by definite outcomes from general level LULCC planning action for Sana'a city utilizing multispectral medium goal satellite information. Our examination shows that the LULC in Sana'a has undergone significant changes from 2015 to 2019.

3.4.1 Random Forest Classifier (RF)

The speed with all test sets is developed to measure the speculation error. Initially intended for AI, the classifier has acquired prominence in the remote detecting local area,

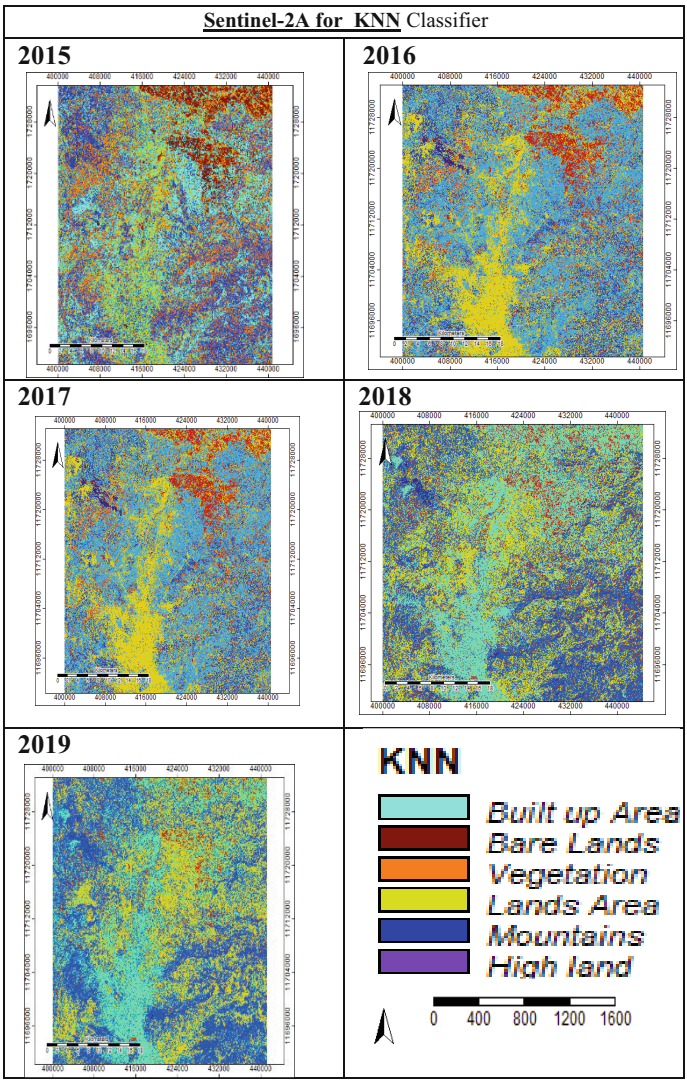

Fig. 10 Group2 of LULC Classification From 2015 To 2019 With **Sentinel-2A for KNN** Classifier

which is applied in distantly detected symbolism characterization because of its high precision. It also accomplishes the appropriate speed required and productive definition. To begin, each tree prepared in the example utilizes arbitrary subsets from the underlying tests. Besides, the ideal split is browsed through the unpruned tree hubs' arbitrarily chosen highlights. Thirdly, every tree develops unbounded [15].

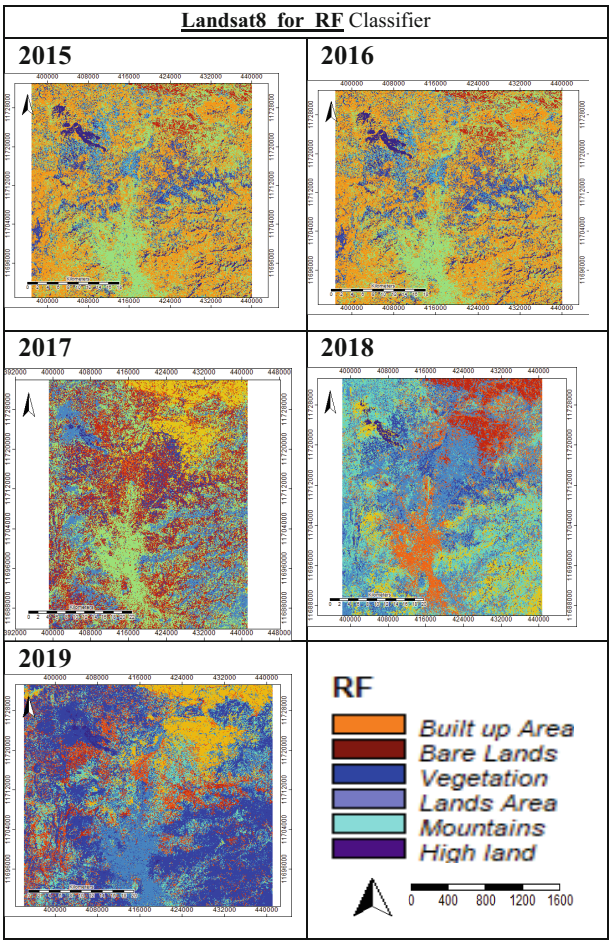

Fig. 11 Group3 of LULC Classification From 2015 To 2019 With **Landsat8 for RF** Classifier

3.4.2 KNN (K-Nearest Neighbor)

It is to discover a collection of k samples from the calibration dataset that are the most similar to unknown models. As a result, the k plays a critical role in its performance for this classifier, and it is the most important tuning parameter. A bootstrap technique was used to calculate the parameter k. This method merely saves the information during the training phase. To explain how it works, use the following algorithm: Step 1: Determine how many neighbors you'll have (K). Step 2: Calculate the Euclidean distance between K neighboring points. Step 3: Determine the K nearest neighbors using the Euclidean distance. Step 4: Among these k neighbors, count the number of data points in each category. Step 5: Assign the newly acquired data points to the class with the most neighbors. Step 6: Our model is now complete. Let's pretend we have a new data point that has to be assigned to the correct category.

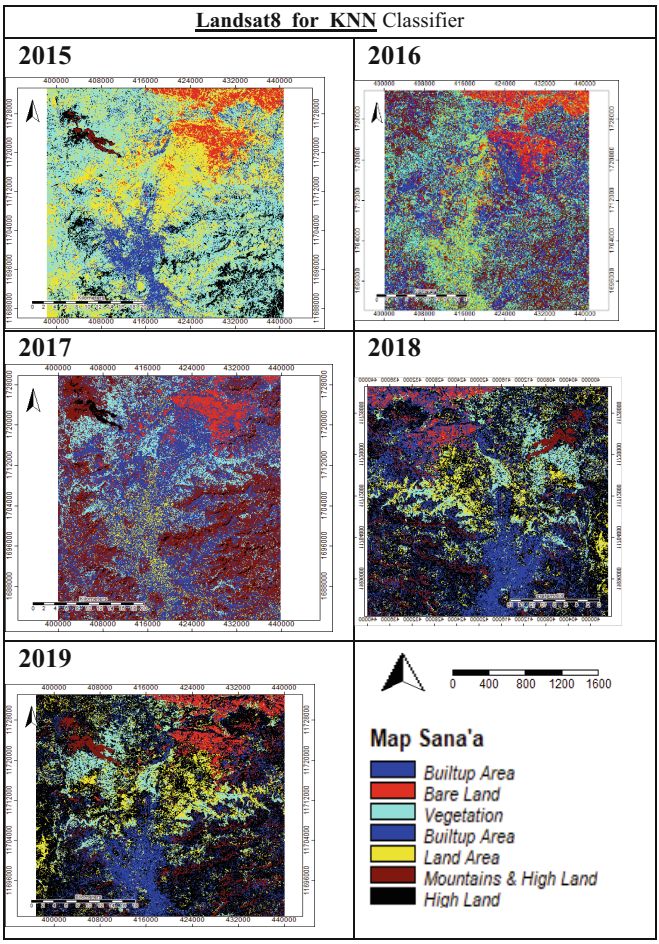

Fig. 12 Group4 of LULC Classification From 2015 To 2019 With **Landsat8 for KNN** Classifier

3.5 Creation of Database and Land Changes Classification

This study used images from Sentinel-2A (10 m) and Landsat 8 multispectral Resolution satellites. The image data was collected from 2015 to 2019, and all photos are from December month. Twelve images are contained each year for Sentinel 2 A. For Landsat8 Satellite, the Spatial Resolution is 30 m. Seven images for respective five years were gathered. The total data size is the number of pictures of multiple years for each satellite 95, as described in (Table 4).

4 Accuracy Assessment

Four measures are available for evaluating classifier performance: Accuracy, confusion matrix, log-loss, and AUC-ROC. This article used the Confusion matrix and A kappa coefficient to estimate classification accuracy. A confusion matrix, also known as an error

Table 4. Creation of Database

SENTINEL-2A Satellite					**Landsat 8 Satellite**				
The sensor is SENTINEL-2A. Resolution is 10m. The time of the season in December.					The sensor is Operational Land Imager (OLI) & Thermal Infrared Sensor (TIRS). Resolution is 30m. The time of the season in December.				
2015	2016	2017	2018	2019	2015	2016	2017	2018	2019
12	12	12	12	12	7	7	7	7	7

matrix, is a table that describes how well a classification model or classifier performs on a set of test data for which the valid values are known. The kappa measurement joins the off-slanting components of the mistake frameworks and addresses arrangement after eliminating the extent of performance anticipated by change. When the Kappa coefficient equals 1, the transaction is in perfect agreement; when it is close to zero, the bargain is no better than expected by chance. A significant number of pixels are taken from the grouped image and contrasted, and a reference guide of more significant position to assess the accuracy of the grouping process. The kappa coefficient goes from 0 to 1, and values higher than 0.7 are considered adequate. At the same time, those equivalent to or lower than 0.4 recognize an external connection between the characterized image and the ground truth. Generally, Kappa values are apparent in (Table 5).

For each class, the confusion matrix, producer's and user's accuracy, overall accuracy, and the accuracy estimate that removes the effect of unexpected change on the accuracy, known as the Kappa statistic, are calculated.

The confusion matrix is straightforward, but the associated nomenclature might be perplexing. A confusion matrix is calculated in this Study through SAGA GIS software. There are four groups for the results of the confusion matrix. Every group containing five categories of the results for five years, 2015 to 2019, is mentioned in (Figs. 13, 14, 15, and 16). The overall accuracy and kappa coefficient calculated in this study are discussed in (Table 6).

Table 5. Strength of Agreement of A kappa coefficient

No.	Kappa Value	Degree of agreement
1	< 0.00	low
2	0.00–0.20	medium
3	0.21–0.40	Good
4	0.41–0.60	Very Good
5	0.61–0.80	Excellence
6	0.80–1.00	Very Excellence

Table 6. Overall accuracy and Kappa coefficient for Sentinel2A satellite with RF & KNN classifier

		RF Classifier				**KNN Classifier**			
		Sentinel2A satellite		Landsat8 satellite		Sentinel2A satellite		Landsat8 satellite	
No	Year	Overall Accuracy	Kappa coefficient	Overall Accuracy	Kappa coefficient	Overall Accuracy	Kappa coefficient	Overall Accuracy	Kappa Coefficient
1	2015	99.87%	0.997470	99.66%	0.045511	83.26%	0.919499	92.90%	0.781132
2	2016	99.92%	0.998937	99.83%	0.997137	91.56%	0.977268	96.34%	0.954044
3	2017	99.78%	0.996582	99.59%	-0.056751	91.49%	0.952622	94.88%	0.794250
4	2018	99.82%	0.996878	99.81%	0.997368	84.56%	0.933182	94.88%	0.780590
5	2019	99.79%	0.996686	99.29%	0.653902	83.83%	0.736954	93.86%	0.781132

5 Results and Discussion

The land changes' results are detailed in Tables 7, 8, 9 and 10. Also, the area under major land-use or land-cover classes was calculated for 2015 to 2019. It is observed that the region has changed during the mentioned period. There are differences in the entire geographic space of the Land use and land cover maps. There has been a persistent reduction in Vegetation & Bare Land and increased land cover with expansion in cropland and developed regions. The part was advancing in urban area density, built-up area, and land presence, and the built-up area fell. The land area expanded, and the built-up area was 30.56% in 2015, 25.27% in 2016, 17.78% in 2017, 28.76% in 2018, and 20.24% in 2019, depending on LULC. They were using Sentinel-2A for RF consideration for the highest accuracy. The Land Use & Land cover classification using RF classifier with Sentinel-2A gave accuracy results higher than Landsat8 f with the same period. But, the KNN classifier type with Sentinel-2A gave less accuracy than Landsat8 with the same period. That means Landsat8 results were better than Sentinel-2A with the same period (Table 11). Since the Sentinel-2A satellite has a 10m resolution, which is efficient for object classification, thus proved good with RF and KNN.

2015

CLASS	High Land	Mountains	Builtup	Land Area	Vegetation	Bare Land	SumUser	AccUser
High Land	0	0	0	0	0	0	250	0
Mountains	1230	0	0	0	0	0	0	
Land Area	0	0	55	0	0	0	120	100
Builtup	0	0	0	0	0	0	44	0
Vegetation	0	0	0	250	0	0	158	0
Bare Land	0	0	0	0	0	0	1235	0
Unclassified	0	0	0	0	0	0	0	0
SumProd	44	55	250	158	1235	120		
AccProd	0	100	0	0	0	100		

2016

CLASS	High Land	Mountains	Builtup	Land Area	Vegetation	Bare Land	SumUser	AccUser
High Land	222	0	0	0	0	0	82	98.78049
Mountains	0	81	0	1	0	0	165	99.39394
Land Area	0	0	164	1	0	0	107	100
Builtup	0	0	0	107	0	0	2075	99.80723
Vegetation	0	0	0	0	2071	4	824	100
Bare Land	0	0	0	0	0	824	58	100
Unclassified	222	0	0	0	0	0	0	0
SumProd	81	164	109	2071	828	58		
AccProd	100	100	98.16514	100	99.51691	100		

2017

CLASS	High Land	Mountains	Builtup	Land Area	Vegetation	Bare Land	SumUser	AccUser
High Land	203	0	0	0	0	0	59	0
Mountains	0	0	0	0	438	0	52	0
Land Area	0	59	0	0	0	0	226	0
Builtup	0	0	52	0	0	0	0	
Vegetation	0	0	0	226	0	0	21	0
Bare Land	0	0	0	0	0	0	614	0
Unclassified	203	0	0	0	0	0	0	0
SumProd	203	672	52	226	439	21		
AccProd	100	0	0	0	0	0		

2018

CLASS	High Land	Mountains	Builtup	Land Area	Vegetation	Bare Land	SumUser	AccUser
High Land	1838	2	0	0	0	1	1841	99.83705
Mountains	3	2178	0	1	0	0	2182	99.81668
Land Area	0	0	205	1	0	0	206	99.51456
Builtup	0	0	0	328	0	0	328	100
Vegetation	0	0	0	1	562	0	563	99.82238
Bare Land	0	0	0	1	0	175	176	99.43182
Unclassified	0	0	0	21	0	0	0	0
SumProd	1841	2180	205	332	562	176		
AccProd	99.83705	99.90826	100	98.79518	100	99.43182		

2019

CLASS	High Land	Mountains	Builtup	Land Area	Vegetation	Bare Land	SumUser	AccUser
High Land	0	0	0	0	0	0	61	100
Mountains	0	0	56	0	0	0	106	100
Land Area	0	0	0	938	0	0	0	
Builtup	0	0	0	0	376	0	128	99.21875
Vegetation	0	0	0	0	0	0	0	
Bare Land	0	637	0	0	0	0	56	100
Unclassified	0	0	0	0	0	344	0	0
SumProd	127	637	56	938	376	0		
AccProd	100	0	100	100	100			

Fig. 13 Group1 of Confusion Matrix Tables to **Landsat8 with RF** Classifier from 2015 To 2019

2015

CLASS	High Land	Mountains	Builtup	Land Area	Vegetation	Bare Land	SumUser	AccUser
High Land	0	0	0	0	0	0	84	85.71429
Mountains	0	0	0	92	0	1	93	98.92473
Land Area	0	0	0	0	55	0	57	96.49123
Builtup	0	0	0	2	0	370	372	99.46237
Vegetation	0	5	43	1	0	0	356	86.23596
Bare Land	0	0	80	1	0	0	112	0
Unclassified	0	0	0	0	0	0	0	0
SumProd	100	77	124	96	58	371		
AccProd	100	93.50649	0	95.83333	94.82759	99.73046		

2016

CLASS	High Land	Mountains	Builtup	Land Area	Vegetation	Bare Land	SumUser	AccUser
High Land	73	0	7	1	0	0	81	90.12346
Mountains	0	158	7	9	1	0	175	90.28571
Land Area	8	1	94	0	0	0	103	91.26214
Builtup	0	4	1	1978	65	0	2048	96.58203
Vegetation	0	1	0	82	761	0	846	89.95272
Bare Land	0	0	0	0	0	58	58	100
Unclassified	0	0	0	0	0	0	0	0
SumProd	81	164	109	2071	828	58		
AccProd	90.12346	96.34146	86.23853	95.50942	91.90821	100		

2017

CLASS	High Land	Mountains	Builtup	Land Area	Vegetation	Bare Land	SumUser	AccUser
High Land	50	0	0	2	0	0	52	96.15385
Mountains	0	225	1	0	0	0	226	99.55752
Land Area	0	1	399	0	5	0	436	91.51376
Builtup	2	0	0	19	0	0	21	90.47619
Vegetation	0	0	0	0	609	0	609	100
Bare Land	0	0	0	0	0	96	96	100
Unclassified	0	0	6	0	0	0	0	0
SumProd	52	226	433	21	614	96		
AccProd	96.15385	99.55752	92.14781	90.47619	99.18567	100		

2018

CLASS	High Land	Mountains	Builtup	Land Area	Vegetation	Bare Land	SumUser	AccUser
High Land	684	1	1	0	0	0	686	99.70846
Mountains	1	8361	11	8	14	0	8395	99.595
Land Area	0	4	21126	1	5	0	21136	99.95269
Builtup	0	2	0	2924	1	0	2927	99.89751
Vegetation	0	0	0	1	2048	0	2049	99.9512
Bare Land	0	0	0	0	0	28	28	100
Unclassified	0	0	0	0	0	0	0	0
SumProd	685	8368	21138	2934	2068	28		
AccProd	99.85402	99.91635	99.94323	99.65917	99.03288	100		

2019

CLASS	High Land	Mountains	Builtup	Land Area	Vegetation	Bare Land	SumUser	AccUser
High Land	445	0	0	0	0	0	445	100
Mountains	0	2353	0	1	1	2	2357	99.83029
Land Area	0	0	45	0	0	0	45	100
Builtup	0	6	0	13952	1	3	13962	99.92838
Vegetation	0	2	0	0	1511	3	1516	99.67019
Bare Land	0	13	0	3	0	6112	6128	99.7389
Unclassified	0	0	0	0	0	0	0	0
SumProd	445	2374	45	13956	1513	6120		
AccProd	100	99.11542	100	99.97134	99.86781	99.86928		

Fig. 14 Group2 of Confusion Matrix Tables to **Landsat8 with KNN** Classifier from 2015 To 2019

2015

CLASS	High Land	Mountains	Builtup	Land Area	Vegetation	Bare Land	SumUser	AccUser
High Land	770	0	0	0	1	0	771	99.8703
Mountains	0	698	0	0	1	0	699	99.85694
Land Area	0	1	4981	1	1	0	4984	99.93981
Builtup	6	7	1	19285	44	0	19343	99.70015
Vegetation	6	0	0	21	44121	3	44151	99.93205
Bare Land	0	0	0	0	2	816	818	99.7555
Unclassified	837	0	0	0	0	0	0	0
SumProd	782	706	4982	19307	44170	819		
AccProd	98.46547	98.86686	99.97993	99.88605	99.88907	99.6337		

2016

CLASS	High Land	Mountains	Builtup	Land Area	Vegetation	Bare Land	SumUser	AccUser
High Land	497	0	1	1	0	0	499	99.5992
Mountains	0	1123	0	1	0	0	1124	99.91103
Land Area	0	0	482	0	0	0	482	100
Builtup	0	0	1	3015	0	0	3016	99.96684
Vegetation	0	1	0	0	258	0	259	99.6139
Bare Land	0	0	0	0	0	1103	1103	100
Unclassified	0	0	0	0	0	0	0	0
SumProd	497	1124	484	3017	258	1103		
AccProd	100	99.91103	99.58678	99.93371	100	100		

2017

CLASS	High Land	Mountains	Builtup	Land Area	Vegetation	Bare Land	SumUser	AccUser
High Land	11513	11	16	17	5	0	11566	99.54176
Mountains	5	3489	1	0	0	0	3495	99.82833
Land Area	2	0	14202	5	1	0	14210	99.9437
Builtup	0	0	0	935	0	0	935	100
Vegetation	1	0	0	0	485	0	486	99.79424
Bare Land	0	0	0	0	0	290	290	100
Unclassified	0	0	0	0	0	0	0	0
SumProd	11523	3500	14219	957	491	290		
AccProd	99.91322	99.68571	99.88044	97.70115	98.778	100		

2018

CLASS	High Land	Mountains	Builtup	Land Area	Vegetation	Bare Land	SumUser	AccUser
High Land	8355	14	6	14	1	0	8392	99.5591
Mountains	6	21124	3	8	0	0	21141	99.91959
Land Area	3	0	2925	2	0	0	2930	99.82935
Builtup	3	0	0	1883	0	0	1886	99.84093
Vegetation	0	0	0	0	160	0	160	100
Bare Land	0	0	0	0	0	28	28	100
Unclassified	0	0	0	0	0	0	0	0
SumProd	8368	21138	2934	1907	161	28		
AccProd	99.84465	99.93377	99.69325	98.74148	99.37888	100		

2019

CLASS	High Land	Mountains	Builtup	Land Area	Vegetation	Bare Land	SumUser	AccUser
High Land	15187	26	9	22	2	0	15248	99.59995
Mountains	2	22921	1	14	0	0	22938	99.92589
Land Area	5	5	4796	2	0	0	4808	99.75042
Builtup	3	0	1	2124	0	0	2128	99.81203
Vegetation	1	0	0	0	210	0	211	99.52607
Bare Land	0	0	0	0	0	45	45	100
Unclassified	0	0	0	0	0	0	0	0
SumProd	15198	22952	4807	2162	212	45		
AccProd	99.92762	99.86494	99.77117	98.24237	99.0566	100		

Fig. 15 Group3 of Confusion Matrix Tables to **Sentinal-2A with RF** Classifier from 2015 To 2019

2015

CLASS	High Land	Mountains	Builtup	Land Area	Vegetation	Bare Land	SumUser	AccUser
High Land	71	0	0	0	0	0	71	100
Mountains	0	497	0	5	0	0	502	99.00398
Land Area	0	0	1123	4	0	0	1127	99.64508
Builtup	0	0	0	253	0	0	253	100
Vegetation	0	0	1	0	3017	2	3020	99.90066
Bare Land	0	0	0	0	0	1101	1101	100
Unclassified	0	0	0	480	0	0	0	0
SumProd	71	497	1124	262	3017	1103		
AccProd	100	100	99.91103	96.56489	100	99.81868		

2016

CLASS	High Land	Mountains	Builtup	Land Area	Vegetation	Bare Land	SumUser	AccUser
High Land	497	0	1	1	0	0	499	99.5992
Mountains	0	1123	0	1	0	0	1124	99.91103
Land Area	0	0	482	0	0	0	482	100
Builtup	0	0	1	3015	0	0	3016	99.96684
Vegetation	0	1	0	0	258	0	259	99.6139
Bare Land	0	0	0	0	0	1103	1103	100
Unclassified	0	0	0	0	0	0	0	0
SumProd	497	1124	484	3017	258	1103		
AccProd	100	99.91103	99.58678	99.93371	100	100		

2017

CLASS	High Land	Mountains	Builtup	Land Area	Vegetation	Bare Land	SumUser	AccUser
High Land	561	1	0	0	0	0	562	99.82206
Mountains	3	11515	20	11	18	0	11567	99.55045
Land Area	0	4	3479	3	0	0	3486	99.7992
Builtup	0	3	1	14205	4	0	14213	99.94371
Vegetation	0	0	0	0	1426	0	1426	100
Bare Land	0	0	0	0	0	290	290	100
Unclassified	0	0	0	0	0	0	0	0
SumProd	564	11523	3500	14219	1448	290		
AccProd	99.46809	99.93057	99.4	99.90154	98.48066	100		

2018

CLASS	High Land	Mountains	Builtup	Land Area	Vegetation	Bare Land	SumUser	AccUser
High Land	684	1	1	0	0	0	686	99.70846
Mountains	1	8361	11	8	14	0	8395	99.595
Land Area	0	4	21126	1	5	0	21136	99.95269
Builtup	0	2	0	2924	1	0	2927	99.89751
Vegetation	0	0	0	1	2048	0	2049	99.9512
Bare Land	0	0	0	0	0	28	28	100
Unclassified	0	0	0	0	0	0	0	0
SumProd	685	8368	21138	2934	2068	28		
AccProd	99.85402	99.91635	99.94323	99.65917	99.03288	100		

2019

CLASS	High Land	Mountains	Builtup	Land Area	Vegetation	Bare Land	SumUser	AccUser
High Land	445	0	0	0	0	0	445	100
Mountains	0	2353	0	1	1	2	2357	99.83029
Land Area	0	0	45	0	0	0	45	100
Builtup	0	6	0	13952	1	3	13962	99.92838
Vegetation	0	2	0	0	1511	3	1516	99.67019
Bare Land	0	13	0	3	0	6112	6128	99.7389
Unclassified	0	0	0	0	0	0	0	0
SumProd	445	2374	45	13956	1513	6120		
AccProd	100	99.11542	100	99.97134	99.86781	99.86928		

Fig. 16 Group4 of Confusion Matrix Tables to **Sentinal-2A with KNN** Classifier from 2015 To 2019

Table 7. Area and Percentages for LULC Using Sentinel-2A for RF from 2015 to 2019

No.	NAME	2015		2016		2017		2018		2019	
		Area, km^2	%	Area, km^2	%	Area, km^2	%	Area, km^2	%	Area, km^2	%
1	High Land	8712800	0.54%	13669300	0.79%	6743200	0.38%	23567000	1.23%	4077900	0.23%
2	Mountains & High Land	900226900	55.33%	279508700	16.05%	742869700	41.85%	734593900	38.41%	714204300	40.33%
3	Land Area Roads& buildings	61831200	3.80%	704028100	40.44%	605930900	34.14%	472178100	24.69%	585212200	33.05%
4	Builtup Area	497245100	30.56%	440027300	25.27%	315670100	17.78%	550033600	28.76%	361557300	20.42%
5	Vegetation	27778600	9.35%	208762600	11.99%	32317600	1.82%	82921500.00%	4.34%	81325800	4.59%
6	Bare Land	131257500	8.07%	95098700	5.46%	71481500	4.03%	49147800	2.57%	24343900	1.37%
7	Total of area =	1627052100	100.00%	1741094700	100.00%	1775013000	100.00%	1912441900	100.00%	1770721400	100.00%

Table 8. Area and Percentages for LULC Using Sentinel-2A for KNN from 2015 to 2019

No.	NAME	2015		2016		2017		2018		2019	
		Area, km^2	%	Area, km^2	%	Area, km^2	Percentage	Area, km^2	%	Area, km^2	%
1	High Land	15952300	1.02%	13162600	0.76%	6782300	0.38%	23465600	1.23%	30886700	1.74%
2	Mountains & High Land	364087100	23.35%	275873200	15.84%	732874600	41.29%	748233400	39.12%	836821700	47.26%
3	Land Area Roads& buildings	688764900	44.17%	704557400	40.47%	616511800	34.73%	465641400	24.35%	233687900	13.20%
4	Builtup Area	374969400	24.05%	449061900	25.79%	312892200	17.63%	540760200	28.28%	465307600	26.28%
5	Vegetation	11811200	0.76%	210669100	12.10%	33643600	1.90%	85667800	4.48%	161504300	9.12%
6	Bare Land	103773000	6.65%	87770400	5.04%	72308700	4.07%	48673500	2.55%	42513300	2.40%
7	Total of area =	1559357900	100.00%	1741094600	100.00%	1775013200	100.00%	1912441900	100.00%	1770721500	100.00%

Table 9. Area and percentages LULC with Landsat8 for KNN from 2015 to 2019

No.	NAME	2015		2016		2017		2018		2019	
		Area, km^2	%	Area, km^2	%	Area, km^2	%	Area, km^2	%	Area, km^2	%
1	High Land	121965300	2.58%	121965300	4.63%	12273300	0.61%	23465600	1.23%	33465600	2.23%
2	Mountains & High Land	1512416700	31.96%	1512416700	53.08%	205126200	10.23%	748233400	39.12%	848233400	40.12%
3	Land Area	232313400	4.91%	232313400	10.58%	588451500	29.36%	465641400	24.35%	565641400	25.35%
4	Builtup Area	1972601100	41.68%	1116102600	18.75%	228424500	11.40%	540760200	28.28%	640760200	29.28%
5	Vegetation	567041400	11.98%	567041400	8.05%	848327400	42.33%	85667800	4.48%	95667800	5.48%
6	Bare Land	326055600	6.89%	326055600	4.92%	121594500	6.07%	48673500	2.55%	58673500	3.55%
7	Total of area =	4732393500	100.00%	1911456900	100.00%	2004197400	100.00%	1912441900	100.00%	3012441900	100.00%

Table 10. Area and Percentages for LULC Using Landsat8 for RF from 2015 To 2019

No.	NAME	2015		2016		2017		2018		2019	
		Area, km^2	%	Area, km^2	%	Area, km^2	%	Area, km^2	%	Area, km^2	%
1	High Land	152003700	7.33%	80561700	4.21%	10071900	0.81%	10184400	0.48%	6527700	0.65%
2	Mountains & High Land	791696700	38.18%	890460900	46.59%	501359400	40.28%	861487200	40.94%	219599100	21.87%
3	Land Area	266358600	12.84%	180999900	9.47%	116273700	9.34%	343812600	16.34%	127650600	12.71%
4	Builtup Area	597589200	28.82%	548289900	28.68%	453569400	36.44%	337429800	16.03%	461995200	46.00%
5	Vegetation	141367500	6.82%	155898900	8.16%	15237000	1.22%	344167200	16.35%	67280400	6.70%
6	Bare Land	124767000	6.02%	55244700	2.89%	148232700	11.91%	207279000	9.85%	121186800	12.07%
7	Total of area =	2073782700	100.00%	1911456000	100.00%	1244744100	100.00%	2104360200	100.00%	1004239800	100.00%

Table 11. Overall accuracy for Sentinel-2A & Landsat8 Satellites from 2015 to 2019 with RF & KNN classifiers

No.	Year	Accuracy LULCC With **RF**		Accuracy LULCC With **KNN**	
		Landsat8	**Sentinel-2A**	**Landsat8**	**Sentinel-2A**
1	2015	99.66%	99.87%	92.90%	83.26%
2	2016	99.83%	99.92%	96.34%	91.56%
3	2017	99.59%	99.78%	94.88%	91.49%
4	2018	99.81%	99.82%	94.88%	84.56%
5	2019	99.29%	99.79%	93.86%	83.83%

6 Conclusion

This Study offered criteria for classification using machine learning with multispectral satellites. It is not enough to select high-resolution data. The classifier's type must also be considered. Classifying land-use changes and land cover requires an integrated study of everything related to classification, focusing on three sides: 1) The type of the satellites. 2) The type characteristics of the classifier chosen are suitable for this satellite. 3) Appropriateness of the typical characteristics of the classifier chosen suitable for this satellite is critical. All of these factors have a role in achieving high-accuracy classification results. According to this Study's findings, the effectiveness of any classification system is mainly dependent on precise knowledge of satellite data, classifier features, and the user's skill. Random forest is observed to be efficient for Sentinel 2A satellite images. The RF classifier may have needed numerous features to achieve acceptable accuracy, which could explain how these results were interpreted. At the same time, KNN provides decent accuracy and performs well with few input feature variables.This study also showed that machine learning is still widely utilized and used today, beating deep learning in features and characteristics despite deep learning's high resolution. Deep learning is more challenging to implement and takes more time than machine learning. The study showed that, without deep learning, we could have classified LULC with a very high resolution using multispectral satellites and conventional machine learning.

References

1. Thanh Noi, P., & Kappas, M. Compare random forest, k-nearest neighbor, and support vector machine classifiers for land cover classification using Sentinel-2 imagery. Sensors, 18(1), 18, (2018).
2. Alshari, E. A., & Gawali, B. W. Evaluation of the Potentials and Challenges of Land Observation Satellites. Global Transitions Proceedings. (2021).
3. https://en.wikipedia.org/wiki/Sentinel-2.
4. https://en.wikipedia.org/wiki/Landsat_8
5. Ming, D., Zhou, T., Wang, M., & Tan, T. Land cover classification using random forest with genetic algorithm-based parameter optimization. Journal of Applied Remote Sensing, 10(3), 035021 , (2016).
6. Zhu, L., Suomalainen, J., Liu, J., Hyyppä, J., Kaartinen, H., & Haggren, H. A Review: Remote Sensing Sensors. Multi-Purposeful Application of Geospatial Data. doi:https://doi.org/10.5772/intechopen.71049, (2018).
7. Alshari, E. A., & Gawali, B. W. Development of classification system for LULC using remote sensing and GIS. Global Transitions Proceedings, 2(1), 8-17, (2021).
8. Tewabe, D., & Fentahun, T. Assessment of land use and disclosure of land change using remote sensing in the Tana Lake basin, northwest Ethiopia. Environmental Science Cogent, 6 (1), 1778998, (2020).
9. Fu, W., Ma, J., Chen, P., & Chen, F. Remote Sensing Satellites for Digital Earth. Manual of Digital Earth, 55–123. doi:https://doi.org/10.1007/978-981-32-9915-3_3, (2019).
10. Vali, A., Comai, S., & Matteucci, M. Deep Learning for Land Use and Land Cover Classification Based on Hyperspectral and Multispectral Earth Observation Data: A Review. Remote Sensing, 12(15), 2495. doi:https://doi.org/10.3390/rs12152495, (2020).
11. Radočaj, D., Obhođaš, J., Jurišić, M., & Gašparović, M. Global Open Data Remote Sensing Satellite Missions for Land Monitoring and Conservation: A Review. Land, 9(11), 402. doi:https://doi.org/10.3390/land9110402, (2020).
12. Sarica, A., Cerasa, A., & Quattrone, A. Random forest algorithm for classifying neuroimaging data in Alzheimer's disease: a systematic review. Frontiers in aging neuroscience, 9, 329., (2017).
13. Johnson, D. M., & Mueller, R. Pre-and within-season crop type classification trained with archival land cover information. Remote Sensing of Environment, 264, 112576, (2021).
14. Loi, D. T., Khac, D. V., Hung, D. N., Dong, N. T., Vinh, D. X., & Weber, C. Using Sentinel-2A and Landsat 8 data, a case study of Cam Pha city-Quang Ninh province, monitoring coastline change. Vietnam Journal of Earth Sciences, 43(3), 249-272, (2021).
15. Dhillon, M. S., Dahms, T., Kübert-Flock, C., Steffan-Dewenter, I., Zhang, J., & Ullmann, T. Spatiotemporal Fusion Modelling Using STARFM: Examples of Landsat 8 and Sentinel-2 NDVI in Bavaria. Remote Sensing, 14(3), 677, (2022).
16. Gu, S., Zhang, R., Luo, H., Li, M., Feng, H., & Tang, X. Improved singan integrated with an attentional mechanism for remote sensing image classification. Remote Sensing, 13(9), 1713, (2021).
17. Ahady, A. B., & Kaplan, G. Classification comparison of Landsat-8 and Sentinel-2 data in Google Earth Engine, study case of the city of Kabul. International Journal of Engineering and Geosciences, 7(1), 24-31, (2022).
18. Aksoy, S., Yildirim, A., Gorji, T., Hamzehpour, N., Tanik, A., & Sertel, E. Assessing the performance of machine learning algorithms for soil salinity mapping in Google Earth Engine platform using Sentinel-2A and Landsat-8 OLI data. Advances in Space Research, 69(2), 1072-1086, (2022).

19. Ai, B., Huang, K., Zhao, J., Sun, S., Jian, Z., & Liu, X. Comparison of Classification Algorithms for Detecting Typical Coastal Reclamation in Guangdong Province with Landsat 8 and Sentinel 2 Images. Remote Sensing, 14(2), 385, (2022).
20. Rumora, L., Miller, M., & Medak, D. Contemporary comparative assessment of atmospheric correction influence on radiometric indices between Sentinel-2A and Landsat 8 imagery. Geocarto International, 36(1), 13-27, (2021).
21. Alhedyan, M. A. Change detection of land use and land cover, using landsat-8 and sentinel-2A images (Doctoral dissertation, University of Leicester), (2021).
22. Ghayour, L., Neshat, A., Paryani, S., Shahabi, H., Shirzadi, A., Chen, W., ... & Ahmad, A. Performance evaluation of sentinel-2 and landsat 8 OLI data for land cover/use classification using a comparison between machine learning algorithms. Remote Sensing, 13(7), 1349 (2021).
23. Deliry, S. I., Avdan, Z. Y., & Avdan, U. Extracting urban impervious surfaces from Sentinel-2 and Landsat-8 satellite data for urban planning and environmental management. Environmental Science and Pollution Research, 28(6), 6572-6586, (2021).
24. Nandasena, W. D. K. V., Brabyn, L., & Serrao-Neumann, S. Using Google Earth Engine to classify unique forest and agroforest classes using Sentinel 2a spectral data topographical features: a Sri Lanka case study. Geocarto International, 1–16, (2021).
25. Sheykhmousa, M., Mahdianpari, M., Ghanbari, H., Mohammadimanesh, F., Ghamisi, P., & Homayouni, S. Support vector machine versus random forest for remote sensing image classification: A meta-analysis and systematic review. IEEE Journal of Selected Topics in Applied Earth Observations and Remote Sensing, 13, 6308–6325. Dou, P., Shen, H., Li, Z., Guan, X., & Huang, W. (2021), (2020).
26. Skakun, S., Vermote, E. F., Artigas, A. E. S., Rountree, W. H., & Roger, J. C. An experimental sky-image-derived cloud validation dataset for Sentinel-2 and Landsat 8 satellites over NASA GSFC. International Journal of Applied Earth Observation and Geoinformation, 95, 102253, (2021).
27. Mitri, G., Nader, M., Abou Dagher, M., & Gebrael, K. Investigating the performance of Sentinel-2A and Landsat 8 imagery mapping shoreline changes. Journal of Coastal Conservation, 24(3), 1-9, (2020).
28. Demirkan, D. Ç., Koz, A., & Düzgün, H. S. Hierarchical classification of Sentinel 2-a images for land use and land cover mapping and its use for the CORINE system. Journal of applied remote sensing, 14(2), 026524, (2020).
29. Mansaray, L. R., Wang, F., Huang, J., Yang, L., & Kanu, A. S. Accuracies of support vector machine and random forest in rice mapping with Sentinel-1A, Landsat-8 and Sentinel-2A datasets. Geocarto International, 35(10), 1088-1108, (2020).
30. Xi, Y., Thinh, N. X., & Li, C. Preliminary comparative assessment of various spectral indices for built-up land derived from Landsat-8 OLI and Sentinel-2A MSI imageries. European Journal of Remote Sensing, 52(1), 240-252 , (2019).
31. Najafi, P., Navid, H., Feizizadeh, B., Eskandari, I., & Blaschke, T. Fuzzy object-based image analysis methods using Sentinel-2A and Landsat-8 data to map and characterize soil surface residue. Remote Sensing, 11(21), 2583, (2019).
32. Chastain, R., Housman, I., Goldstein, J., Finco, M., & Tenneson, K. Empirical cross sensor comparison of Sentinel-2A and 2B MSI, Landsat-8 OLI, and Landsat-7 ETM+ top of atmosphere spectral characteristics over the conterminous United States. Remote sensing of environment, 221, 274-285, (2019).
33. Çavur, M., Duzgun, H. S., Kemeç, S., & Demirkan, D. C. Land use and land cover classification of Sentinel 2-A: St Petersburg case study. The International Archives of Photogrammetry, Remote Sensing and Spatial Information Sciences, 42, 13-16, (2019).
34. Varade, D., Sure, A., & Dikshit, O. Potential of Landsat-8 and Sentinel-2A composite for land use land cover analysis. Geocarto International, 34(14), 1552-1567, (2019).

35. Liu, Y., Gong, W., Hu, X., & Gong, J. (2018). Forest type identification with random forest using Sentinel-1A, Sentinel-2A, multi-temporal Landsat-8, and DEM data. Remote Sensing, 10(6), 946.
36. Al-shalabi, M., Pradhan, B., Billa, L., Mansor, S., & Althuwaynee, O. F. Manifestation of remote sensing data in modeling urban sprawl using the SLEUTH model and brute force calibration: a case study of Sana'a city, Yemen. Journal of the Indian Society of Remote Sensing, 41(2), 405-416, (2013).
37. Abdelkareem, O. E. A., Elamin, H. M. A., Eltahir, M. E. S., Adam, H. E., Elhaja, M. E., Rahamtalla, A. M., ... & Elmar, C. Accuracy assessment of land use land cover in umabdalla natural reserved forest, South Kordofan, Sudan. Int J Agric Environ Sci, 3(1), 5–9. (2018).